# Magnetohydrodynamic instability of a high magnetic shear layer with a finite curvature radius

Cite as: Physics of Plasmas **9**, 401 (2002); https://doi.org/10.1063/1.1432698
Submitted: 12 June 2001 . Accepted: 30 October 2001 . Published Online: 22 January 2002

**Irina L. Arshukova, Nikolai V. Erkaev, and Helfried K. Biernat**

# Magnetohydrodynamic instability of a high magnetic shear layer with a finite curvature radius

Irina L. Arshukova and Nikolai V. Erkaev
*Institute of Computational Modelling, Russian Academy of Sciences, Krasnoyarsk 660036, Russia*

Helfried K. Biernat
*Space Research Institute, Austrian Academy of Sciences, Schmiedlstrasse 6, A–8042 Graz, Austria*

(Received 12 June 2001; accepted 30 October 2001)

This article deals with the magnetohydrodynamic instability of a thin layer which is characterized by a high magnetic shear, a constant curvature radius, and a plasma velocity shear. The magnetic field and the plasma parameters are considered to be piecewise constant inside the layer and in the regions adjacent to the layer. The plasma parameters and the magnetic field are assumed to obey the ideal incompressible magnetohydrodynamics. Fourier analysis is used to calculate small perturbations of the magnetic field and plasma parameters near the layer in linear approximation. The instability growth rate is obtained as a function of different parameters: the magnetic shear angle, the velocity direction angle, the tangential plasma velocity, the layer thickness, the wave number, and the curvature radius. The resulting instability is a mixture of interchange and Kelvin–Helmholtz instabilities on a surface with nonzero curvature. For a fixed velocity shear and curvature radius, the instability growth has a maximum in the case of antiparallel magnetic fields (maximal magnetic shear). This growth rate is an increasing function of the tangential velocity component perpendicular to the magnetic field, and a decreasing function of the velocity component along the magnetic field. The instability is stronger for smaller curvature radius. © *2002 American Institute of Physics.* [DOI: 10.1063/1.1432698]

## I. INTRODUCTION

The interchange instability is similar in nature to the Rayleigh–Taylor instability in classic hydrodynamics, where the magnetic tension plays the role of an effective gravitational force.[1–3] There are many aspects of laboratory and space plasma where this instability is important. In space plasma there exist structures which have thin, curved boundary layers separating magnetic fields and plasmas of different origin. Magnetospheres of planets and magnetic clouds are typical examples of such structures.

In particular, the interchange instability was proposed as an important process[3,4] occurring at the Earth's magnetospheric boundary (magnetopause). The reason for this instability is the fact that the plasma pressure should have a local maximum which coincides with the magnetic pressure minimum in the layer separating the antiparallel magnetic fields. For simplicity, the authors[3,4] assumed a tangential discontinuity separating the magnetosheath plasma from the enhanced pressure region in the magnetopause. Applying an incompressible magnetohydrodynamic (MHD) model to the tangential discontinuity, they estimated the instability growth rate as a function of the curvature radius and the shear angle. Concerning this instability problem, there are two important facts which have to be taken into account: A finite thickness of the layer and a velocity shear.

It was shown in Ref. 5 that the finite thickness of the layer is an important parameter which substantially affects the interchange instability growth rate. The velocity shear is of large importance because it drives the Kelvin–Helmholtz instability[6] and thus has a strong influence on the interchange instability.

The aim of our paper is to study the interchange instability of the layer with a high magnetic shear taking into account the plasma velocity directed arbitrarily along the layer, as well as a finite thickness of the curved layer.

## II. STATEMENT OF PROBLEM

With regard to the Kelvin–Helmhotz instability, a three-layered model consisting of three plasma regions (the magnetosheath, the boundary layer, and the magnetosphere) was introduced by Lee *et al.*[7] and Uberoi.[8] We use a similar model to study the interchange instability of a thin layer with a finite curvature radius. This model allows us to study not only the finite thickness effect on the instability growth rate but also magnetic angle effects.

We consider a thin layer of the thickness $2a$ with two idealized sharp boundaries: The first $(F_1)$ is that with contact with region I and the second $(F_2)$ is that of contact with region II (see Fig. 1). The magnetic fields in regions I and II are denoted by the vectors $\mathbf{B}_1$ and $\mathbf{B}_2$, respectively. The magnetic field inside the layer, $\mathbf{B}_0$, is directed between the vectors $\mathbf{B}$ and determined as the vector average, $\mathbf{B}_0=(\mathbf{B}_1+\mathbf{B}_2)/2$. The direction of the plasma flow is determined by the angle $\alpha$ with respect to the magnetic field vector $\mathbf{B}_2$.

To describe the temporal and spatial variations of the magnetic field and plasma parameters resulting from small perturbations of the boundaries $F_1$ $[x_1=f_1(y,z,t)]$ and $F_2$ $[x_2=f_2(y,z,t)]$, we use the ideal magnetohydrodynamic (MHD) equations for an incompressible plasma[6]

 

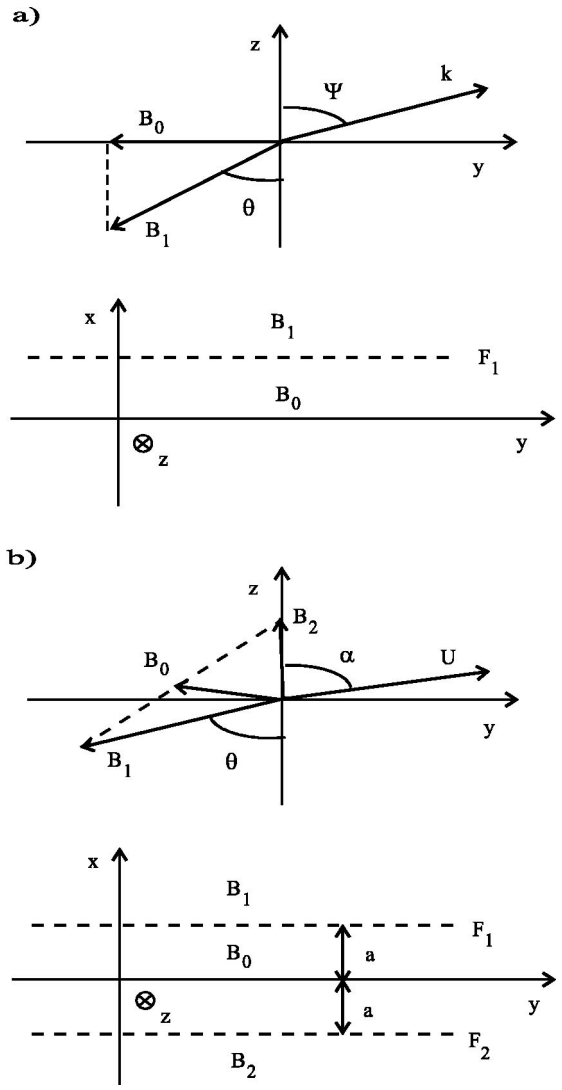


FIG. 1. Geometrical illustrations: (a) corresponds to the model of Rezenov and Maltsev (Ref. 3) and (b) corresponds to our model.

$$\frac{\partial \mathbf{U}}{\partial t}+(\mathbf{U}\cdot\nabla)\,\mathbf{U}+\frac{1}{\rho}\nabla(P)=\frac{1}{4\pi\rho}(\mathbf{B}\cdot\nabla)\,\mathbf{B}, \tag{1}$$

$$\frac{\partial \mathbf{B}}{\partial t}=\nabla\times[\mathbf{U}\times\mathbf{B}],\quad \nabla\cdot\mathbf{B}=0, \tag{2}$$

$$\nabla\cdot\mathbf{U}=0. \tag{3}$$

Here $\rho,\mathbf{U},P,\mathbf{B}$ are the density, velocity, total pressure, and the magnetic field strength, respectively.

Assuming $F_1$ and $F_2$ to be tangential discontinuities, we have no-flow conditions for the normal components of the velocity

$$(\mathbf{U}_{1,2}-\mathbf{D})\cdot\hat{\mathbf{N}}=(\mathbf{U}_0-\mathbf{D})\cdot\hat{\mathbf{N}}=0, \tag{4}$$

where $\mathbf{D}$ is the speed of the boundary surface and $\hat{\mathbf{N}}$ is the unit vector normal to the boundary surface.

In addition, we have balance of the total pressure at both boundaries

$$P_1=P_0,\ \text{for } x=a;\quad P_2=P_0,\ \text{for } x=-a. \tag{5}$$

Hereafter, subscripts ''1, 0, 2'' denote quantities corresponding to the different regions: region I, the layer region, and region II, respectively.

Generally, the surface of the layer is characterized by two main local curvature radii, $R_y$ and $R_z$. In a small neighborhood of the chosen point on the surface, we introduce a local coordinate system related to this surface. The two coordinates $y$ and $z$ are the distances along the geodetic lines on the surface with curvature radii $R_y$ and $R_z$, respectively. The third coordinate $x$ is the distance along the normal to the surface.

We introduce small perturbations of the magnetic field and plasma parameters

$$\mathbf{B}=\mathbf{B}^*+\mathbf{b},\quad P=P^*+p,\quad \mathbf{U}=\mathbf{U}^*+\mathbf{u},$$

where $|\mathbf{b}|\ll|\mathbf{B}|$, $p\ll P$, $|\mathbf{u}|\ll|\mathbf{U}|$.

Assuming that the density of the plasma is constant and that the components $B_x^*$ of the magnetic fields and the components $U_x^*$ of the velocities are equal to zero, we obtain from (1)–(3) the following equations in linear approximation:

$$\frac{\partial u_x}{\partial t}+(\mathbf{U}^*\cdot\nabla^*)u_x-2\left(\frac{U_y^*u_y}{q_yR_y}+\frac{U_z^*u_z}{q_zR_z}\right)+\frac{1}{\rho}\frac{\partial p}{\partial x}$$
$$=\frac{1}{4\pi\rho}\left[(\mathbf{B}^*\cdot\nabla^*)b_x-2\left(\frac{B_y^*b_y}{q_yR_y}+\frac{B_z^*b_z}{q_zR_z}\right)\right], \tag{6}$$

$$\frac{\partial u_y}{\partial t}+(\mathbf{U}^*\cdot\nabla^*)u_y+\frac{U_y^*u_x}{q_yR_y}+\frac{1}{q_y\rho}\frac{\partial p}{\partial y}$$
$$=\frac{1}{4\pi\rho}\left((\mathbf{B}^*\cdot\nabla^*)b_y+\frac{B_y^*b_x}{q_yR_y}\right), \tag{7}$$

$$\frac{\partial u_z}{\partial t}+(\mathbf{U}^*\cdot\nabla^*)u_z+\frac{U_z^*u_x}{q_zR_z}+\frac{1}{q_z\rho}\frac{\partial p}{\partial z}$$
$$=\frac{1}{4\pi\rho}\left((\mathbf{B}^*\cdot\nabla^*)b_z+\frac{B_z^*b_x}{q_zR_z}\right), \tag{8}$$

$$\frac{\partial P^*}{\partial x}=-\frac{1}{4\pi}\left(\frac{B_y^{*\,2}}{R_y}+\frac{B_z^{*\,2}}{R_z}\right)+\rho\left(\frac{U_y^{*\,2}}{R_y}+\frac{U_z^{*\,2}}{R_z}\right), \tag{9}$$

$$\nabla\cdot\mathbf{u}=0,\quad \nabla\cdot\mathbf{b}=0. \tag{10}$$

Here, $\nabla^*$ is a vector operator defined as

$$\nabla^*=\left(\frac{\partial}{\partial x},\frac{1}{q_y}\frac{\partial}{\partial y},\frac{1}{q_z}\frac{\partial}{\partial z}\right),$$

where $q_y$ and $q_z$ are the metric coefficients related to the curvature $q_y=1+x/R_y$ and $q_z=1+x/R_z$. To simplify the problem, we incorporate only the first-order terms with respect to the curvature $\sim 1/R_y$, $\sim 1/R_z$.

Initially, the plasma is assumed to satisfy the steady-state condition and thus the gradient of the total pressure is assumed to compensate the magnetic tension and to support the normal centrifugal acceleration of the plasma flowing around the curved surface. Therefore, the initial total pressure is considered to be a function of the normal distance $x$ and can be linearized near the surface as follows:

$$P=\Pi_0-\frac{1}{4\pi}\left(\frac{B_y^{*2}}{R_y q_y}+\frac{B_z^{*2}}{R_z q_z}\right)x+\rho\left(\frac{U_y^{*2}}{R_y q_y}+\frac{U_z^{*2}}{R_z q_z}\right)x, \tag{11}$$

where $\Pi_0$ is a constant parameter. The variation of the total pressure determined by (11) is caused by the magnetic field tension and the centrifugal force.

From (2), (3) we obtain in linear approximation

$$\frac{\partial b_x}{\partial t}=(\mathbf{B}^*\cdot\nabla^*)u_x-(\mathbf{U}^*\cdot\nabla^*)b_x, \tag{12}$$

$$\frac{\partial b_y}{\partial t}=(\mathbf{B}^*\cdot\nabla^*)u_y-(\mathbf{U}^*\cdot\nabla^*)b_y+(u_xB_y^*-b_xU_y^*)\frac{1}{q_y R_y}, \tag{13}$$

$$\frac{\partial b_z}{\partial t}=(\mathbf{B}^*\cdot\nabla^*)u_z-(\mathbf{U}^*\cdot\nabla^*)b_z+(u_xB_z^*-b_xU_z^*)\frac{1}{q_z R_z}, \tag{14}$$

$$\frac{\partial(q_yq_zu_x)}{\partial x}+\frac{\partial(q_zu_y)}{\partial y}+\frac{\partial(q_yu_z)}{\partial z}=0. \tag{15}$$

For simplicity, we consider the two curvature radii to be equal to each other, $R_y=R_z=R$.

For computational convenience, we introduce the dimensionless parameters

$$\tilde{x}=x/a,\quad \mathbf{K}=\mathbf{k}\cdot a,\quad r=R/a,\quad \tilde{\rho}_i=\rho_i/\rho_1,$$

$$\mathbf{H}_i=\mathbf{B}_i^*/B_2^*,\quad \mathbf{h}_i=\mathbf{b}_i/B_2^*,\quad \mathbf{V}_i=\mathbf{U}_i^*\cdot\sqrt{4\pi\rho_1}/B_2^*,$$

$$\mathbf{v}_i=\mathbf{u}_i\cdot\sqrt{4\pi\rho_1}/B_2^*,$$

$$\tilde{\omega}=\omega\cdot\sqrt{4\pi\rho_1}a/B_2^*,\quad \tilde{p}=p\cdot 4\pi/B_2^{*2}. \tag{16}$$

We use a dimensionless small parameter $\varepsilon=1/kR=1/Kr$ that is treated in linear approximation.

We assume the coefficients of the linearized system to be constant. In such a case we can apply the usual Fourier method to solve our linear MHD problem. Thus, considering all perturbations to be proportional to the complex exponential function $\exp(i(\mathbf{K}\cdot\mathbf{s}-\tilde{\omega}t))$, where $\mathbf{s}$ is a two-dimensional vector in the plane $(yz)$, we obtain from (6)–(10)

$$-i\,q\,\tilde{\omega}\,v_{ix}+i\,(\mathbf{V}_i\cdot\mathbf{K})v_{ix}-2\,\varepsilon\,K(\mathbf{V}_i\cdot\mathbf{v}_i)+\frac{q}{\tilde{\rho}_i}\frac{\partial\tilde{p}_i}{\partial\tilde{x}}$$

$$=\frac{1}{\tilde{\rho}_i}\{i\,(\mathbf{H}_i\cdot\mathbf{K})\,h_{ix}-2\,\varepsilon\,K(\mathbf{H}_i\cdot\mathbf{h}_i)\},$$

$$-i\,q\,\tilde{\omega}\,v_{iy}+i\,(\mathbf{V}_i\cdot\mathbf{K})v_{iy}+\varepsilon\,K(V_{iy}v_{ix})+\frac{i\,K_y}{\tilde{\rho}_i}\tilde{p}_i$$

$$=\frac{1}{\tilde{\rho}_i}\{i\,(\mathbf{H}_i\cdot\mathbf{K})\,h_{iy}+\varepsilon\,K(H_{iy}h_{ix})\},$$

$$-i\,q\,\tilde{\omega}\,v_{iz}+i(\mathbf{V}_i\cdot\mathbf{K})\,v_{iz}+\varepsilon K(V_{iz}v_{ix})+\frac{i\,K_z}{\tilde{\rho}_i}\tilde{p}_i$$

$$=\frac{1}{\tilde{\rho}_i}\{i\,(\mathbf{H}_i\cdot\mathbf{K})\,h_{iz}+\varepsilon\,K(H_{iz}h_{ix})\}, \tag{17}$$

where $q=q_y=q_z=1+\varepsilon\,K\,\tilde{x}$.

In dimensionless form, Eq. (11) can be rewritten as

$$\tilde{P}_i=\tilde{\Pi}_{i0}-\varepsilon\,\frac{K\,\tilde{x}}{q}(H_i^2-\tilde{\rho}_iV_i^2). \tag{18}$$

After normalization, the system of the equations (12)–(15) yields

$$-i\,q\,\tilde{\omega}\,h_{ix}=i\,(\mathbf{H}_i\cdot\mathbf{K})\,v_{ix}-i\,(\mathbf{V}_i\cdot\mathbf{K})\,h_{ix},$$

$$-i\,q\,\tilde{\omega}\,h_{iy}=i\,(\mathbf{H}_i\cdot\mathbf{K})\,v_{iy}-i\,(\mathbf{V}_i\cdot\mathbf{K})\,h_{iy}+\varepsilon\,K\,(v_{ix}H_{iy}-h_{ix}V_{iy}),$$

$$-i\,q\,\tilde{\omega}\,h_{iz}=i\,(\mathbf{H}_i\cdot\mathbf{K})\,v_{iz}-i\,(\mathbf{V}_i\cdot\mathbf{K})\,h_{iz}+\varepsilon\,K\,(v_{ix}H_{iz}-h_{ix}V_{iz}), \tag{19}$$

$$-i\,\frac{\partial v_{ix}}{\partial\tilde{x}}+K_yv_{iy}+K_zv_{iz}-2\varepsilon K(iv_{ix})=0. \tag{20}$$

Using the continuity equation (20) together with Eqs. (17) and (19), we obtain a differential equation for pressure

$$-(1+\varepsilon K\tilde{x})\frac{\partial^2\tilde{p}_i}{\partial\tilde{x}^2}+\varepsilon d_i\frac{\partial\tilde{p}_i}{\partial\tilde{x}}+K^2\tilde{p}_i=0, \tag{21}$$

where

$$d_i=K\frac{4(\mathbf{H}_i\cdot\mathbf{K})^2/\tilde{\rho}_i-3W_i^2+\tilde{\omega}^2-(\mathbf{V}_i\cdot\mathbf{K})^2}{W_i^2-(\mathbf{H}_i\cdot\mathbf{K})^2/\tilde{\rho}_i},$$

$$W_i=\tilde{\omega}-(\mathbf{V}_i\cdot\mathbf{K}).$$

## III. INSTABILITY OF A TANGENTIAL DISCONTINUITY

We start off with the instability problem for one discontinuity which is similar to that studied by Rezenov and Maltsev.[3] This concerns the interchange instability of just one boundary $F_1$ separating the magnetic field in region I from that inside the layer. Under the consideration of zero plasma velocity and constant density, the dimensionless differential equation for the pressure (21) can be written in the form

$$\frac{\partial^2\tilde{p}_i}{\partial\tilde{x}^2}+2\,\varepsilon\,K\frac{2(\mathbf{H}_i\cdot\mathbf{K})^2-\tilde{\rho}_i\tilde{\omega}^2}{(\mathbf{H}_i\cdot\mathbf{K})^2-\tilde{\rho}_i\tilde{\omega}^2}\frac{\partial\tilde{p}_i}{\partial\tilde{x}}-K^2\tilde{p}_i=0. \tag{22}$$

This equation has exponential solutions which are decreasing functions of the distance from the discontinuity

$$\tilde{p}_1 = c_1 \exp(-K\tilde{x})\left\{1+\frac{\varepsilon}{4}[(2d_1+K)\tilde{x}+K^2\tilde{x}^2)] + O(\varepsilon^2)\right\},$$

$$\tilde{p}_0 = c_0 \exp(K\tilde{x})\left\{1+\frac{\varepsilon}{4}[(2d_0+K)\tilde{x}-K^2\tilde{x}^2)] + O(\varepsilon^2)\right\}. \quad (23)$$

Here, $d_i = -2K[2(\mathbf{H}_i\cdot\mathbf{K})^2-\tilde{\rho}_i\tilde{\omega}^2]/[(\mathbf{H}_i\cdot\mathbf{K})^2-\tilde{\rho}_i\tilde{\omega}^2]$; $c_1$, $c_0$ are constants. Thus, all perturbations are localized to the vicinity of the unstable boundary.

From the boundary conditions (4) and (5) we get

$$i v_{1x} = \tilde{\omega} f_1, \quad i v_{0x} = \tilde{\omega} f_1,$$

$$\tilde{p}_1 - \frac{H_1^2}{r} f_1 = \tilde{p}_0 - \frac{H_0^2}{r} f_1. \quad (24)$$

From Eqs. (17), (19), (24), we derive the following system:

$$((\mathbf{H}_1\cdot\mathbf{K})^2-\tilde{\rho}_1\tilde{\omega}^2)\, f_1 = \left(Q_1\tilde{p}_1 - \frac{\partial\tilde{p}_1}{\partial\tilde{x}}\right),$$

$$((\mathbf{H}_0\cdot\mathbf{K})^2-\tilde{\rho}_0\tilde{\omega}^2)\, f_1 = \left(Q_0\tilde{p}_0 - \frac{\partial\tilde{p}_0}{\partial\tilde{x}}\right),$$

$$\tilde{p}_1 - \tilde{p}_0 = \varepsilon K (H_1^2 - H_0^2)\, f_1, \quad (25)$$

where $Q_i = -\varepsilon\, 2K(\mathbf{H}_i\cdot\mathbf{K})^2/[(\mathbf{H}_i\cdot\mathbf{K})^2-\tilde{\rho}_i\tilde{\omega}^2]$. And finally, we obtain the following algebraic equation for the growth rate of instability:

$$\frac{(\mathbf{H}_1\cdot\mathbf{K})^2-\tilde{\rho}_1\,\tilde{\omega}^2}{Q_1+K-\frac{\varepsilon}{4}(2\,d_1+K)} - \frac{(\mathbf{H}_0\cdot\mathbf{K})^2-\tilde{\rho}_0\,\tilde{\omega}^2}{Q_0-K-\frac{\varepsilon}{4}(2\,d_0+K)} = \varepsilon K (H_1^2-H_0^2). \quad (26)$$

This equation determines the growth rate of instability of the one boundary as a function of the direction of the magnetic field in region I (angle $\theta$), a wave number ($k$), and a local curvature radius of the boundary ($R$). This dispersion equation can be transformed into the form suitable for the analysis

$$\tilde{\omega}^2\cdot\left\{\tilde{\rho}_1\left(1-\frac{3}{4}\varepsilon\right)+\tilde{\rho}_0\left(1+\frac{3}{4}\varepsilon\right)\right\} = -\varepsilon K^2(H_1^2-H_0^2)+(\mathbf{H}_1\cdot\mathbf{K})^2\left\{1+\frac{\varepsilon}{4}\right\} + (\mathbf{H}_0\cdot\mathbf{K})^2\left\{1-\frac{\varepsilon}{4}\right\}. \quad (27)$$

In the right-hand side, there are two terms which are in concurrence: The first one is related with the interchange instability effect, and the second one plays a stabilizing role when the wave vector is not exactly perpendicular to the magnetic field. The instability growth rate is largest when the wave vector is perpendicular to the magnetic field vectors $\mathbf{B}_1$ and $\mathbf{B}_0$. But, this is possible only in the case of collinear magnetic vectors $\mathbf{B}_0$ and $\mathbf{B}_1$.

In the particular case $(\mathbf{H_1}\cdot\mathbf{k})=0,(\mathbf{H_0}\cdot\mathbf{k})=0$, the dispersion equation can be simplified to

$$\tilde{\omega}^2\cdot\left\{\tilde{\rho}_1\left(1-\frac{3}{4}\varepsilon\right)+\tilde{\rho}_0\left(1+\frac{3}{4}\varepsilon\right)\right\} = \varepsilon K^2(H_0^2-H_1^2). \quad (28)$$

Comparing Eqs. (27) and (28), one can see that the instability growth rate has a nonregular asymptotic dependence on the small parameter $\varepsilon$. This dependence is different in the cases of collinear ($\sim\sqrt{\varepsilon}$) and noncollinear ($\sim\varepsilon$) magnetic fields.

The frequency determined by Eqs. (27) and (28) is pure imaginary, and thus instability produces nonoscillatory modes which grow exponentially. A real part of frequency appears when a nonzero tangential component of the plasma velocity is taken into account.

## IV. INSTABILITY OF A LAYER

In this section we study the interchange instability of a thin layer bounded by two tangential discontinuities. A finite thickness of the layer and a nonzero velocity of the plasma flow are taken into account.

We seek a solution of Eq. (21) in an exponential form

$$\tilde{p}_i = C_i(\tilde{x})\exp(\kappa_i^0\tilde{x}) = (C_i^0+\varepsilon C_i^1(\tilde{x}))\exp(\kappa_i^0\tilde{x}).$$

Therefore, we have exponential solutions for $\tilde{p}$ in three regions. In the regions above $F_1$ and below $F_2$ (see Fig. 1), the perturbations of the total pressure are given by the following equations:

$$\tilde{p}_1 = c_1\exp(-K\tilde{x})\left\{1+\frac{\varepsilon}{4}[(2d_1+K)\tilde{x}+K^2\tilde{x}^2] + O(\varepsilon^2)\right\},$$

$$\tilde{p}_2 = c_2\exp(K\tilde{x})\left\{1+\frac{\varepsilon}{4}[(2d_2+K)\tilde{x}-K^2\tilde{x}^2]+O(\varepsilon^2)\right\}. \quad (29)$$

In the region between $F_1$ and $F_2$ the solution for the total pressure is a combination of two exponential functions

$$\tilde{p}_0 = c_{01}\exp(-K\tilde{x})\left\{1+\frac{\varepsilon}{4}[(2d_0+K)\tilde{x}+K^2\tilde{x}^2] + O(\varepsilon^2)\right\} + c_{02}\exp(K\tilde{x})\left\{1+\frac{\varepsilon}{4}[(2d_0+K)\tilde{x} - K^2\tilde{x}^2]+O(\varepsilon^2)\right\}. \quad (30)$$

Here, $c_1, c_2, c_{01}$, and $c_{02}$ are constants.

In dimensionless form, the linearized conditions for the total pressure and velocity are

at $\tilde{x}=1$:

$$\tilde{p}_1-\varepsilon K(H_1^2-\tilde{\rho}_1V_1^2)=\tilde{p}_0-\varepsilon K(H_0^2-\tilde{\rho}_0V_0^2),$$

$$iv_{1x}=\tilde{\omega}\tilde{f}_1-(\mathbf{V}_1\cdot\mathbf{K})(1-\varepsilon K\tilde{x})\tilde{f}_1,$$

$$iv_{0x}=\tilde{\omega}\tilde{f}_1-(\mathbf{V}_0\cdot\mathbf{K})(1-\varepsilon K\tilde{x})\tilde{f}_1;$$

at $\tilde{x}=-1$:

$$\tilde{p}_2+\varepsilon K(H_2^2-\tilde{\rho}_2V_2^2)=\tilde{p}_0+\varepsilon K(H_0^2-\tilde{\rho}_0V_0^2),$$

$$iv_{2x}=\tilde{\omega}\tilde{f}_2-(\mathbf{V}_2\cdot\mathbf{K})(1-\varepsilon K\tilde{x})\tilde{f}_2,$$

$$iv_{0x}=\tilde{\omega}\tilde{f}_2-(\mathbf{V}_0\cdot\mathbf{K})(1-\varepsilon K\tilde{x})\tilde{f}_2. \tag{31}$$

Finally, we obtain from Eqs. (17)–(19), (29)–(31) a linear algebraic system for the parameters $c_1$, $c_{01}$, $c_{02}$, $c_2$, $\tilde{f}_1$, and $\tilde{f}_2$

$$L_1^1\tilde{f}_1=A_{1\,1}^1c_1\exp(-K),$$

$$L_0^1\tilde{f}_1=A_{0\,1}^1c_{01}\exp(-K)+A_{0\,2}^1c_{02}\exp(K),$$

$$L_0^2\tilde{f}_2=A_{0\,1}^2c_{01}\exp(K)+A_{0\,2}^2c_{02}\exp(-K),$$

$$L_2^2\tilde{f}_2=A_{2\,2}^2c_2\exp(-K),$$

$$c_1\exp(-K)\,g_{1\,1}^1=c_{01}\exp(-K)\,g_{0\,1}^1+c_{02}\exp(K)\,g_{0\,2}^1+\varepsilon K(H_1^2-H_0^2)\tilde{f}_1-\varepsilon K(\tilde{\rho}_1V_1^2-\tilde{\rho}_0V_0^2)\tilde{f}_1,$$

$$c_2\exp(-K)\,g_{2\,2}^2=c_{01}\exp(K)\,g_{0\,1}^2+c_{02}\exp(-K)\,g_{0\,2}^2+\varepsilon K(H_2^2-H_0^2)\tilde{f}_2-\varepsilon K(\tilde{\rho}_2V_2^2-\tilde{\rho}_0V_0^2)\tilde{f}_2, \tag{32}$$

where

$$W_i=\tilde{\omega}-(\mathbf{V}_i\cdot\mathbf{K}),\quad x_1=1,\quad x_2=-1,$$

$$L_i^j=\{(\mathbf{H}_i\cdot\mathbf{K})^2/\tilde{\rho}_i-W_i^2\}\left\{1+\varepsilon K x_j\frac{\tilde{\omega}+(\mathbf{V}_i\cdot\mathbf{K})}{W_i}\right\},$$

$$d_i=K\frac{4(\mathbf{H}_i\cdot\mathbf{K})^2/\tilde{\rho}_i-3W^2+\tilde{\omega}^2-(\mathbf{V}_i\cdot\mathbf{K})^2}{W^2-(\mathbf{H}_i\cdot\mathbf{K})^2/\tilde{\rho}_i},$$

$$g_{i\,1}^j=1+\frac{\varepsilon}{4}[(2d_i+k)x_j+K^2x_j^2],$$

$$g_{i\,2}^j=1+\frac{\varepsilon}{4}[(2d_i+k)x_j-K^2x_j^2],$$

$$A_{i\,1}^j=\left\{-Kg_{i\,1}^j+\frac{\varepsilon}{4}(2d_i+K+2K^2x_j)\right\}/\tilde{\rho}_i,$$

$$A_{i\,2}^j=\left\{Kg_{i\,2}^j+\frac{\varepsilon}{4}(2d_i+K-2K^2x_j)\right\}/\tilde{\rho}_i. \tag{33}$$

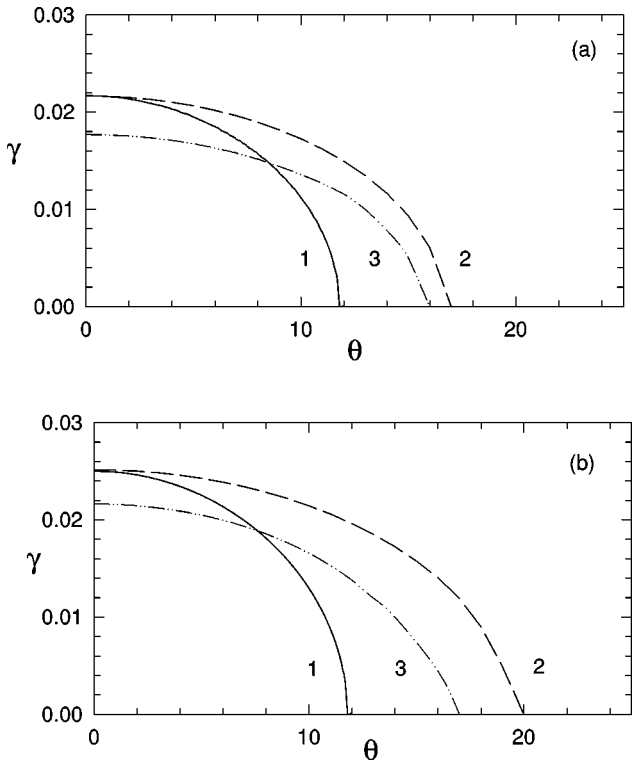


FIG. 2. Instability growth rate versus magnetic shear angle, $ka=0.15$, $R/a=160$, $U_1=U_2=0$. The curve 1 corresponds to Rezenov and Maltsev (Ref. 3), and the curves (2) and (3) are obtained in our models with one and two boundaries, respectively. The plot (a) corresponds to the case of equal densities, $\tilde{\rho}_1=\tilde{\rho}_0=\tilde{\rho}_2=1$, and the plot (b) corresponds to the case of different densities, $\tilde{\rho}_1=1$, $\tilde{\rho}_0=0.5$, $\tilde{\rho}_2=0.1$.

The dispersion equation is determined from the usual condition of a zero determinant for the linear algebraic system (32). The numerical solution of this dispersion equation is analyzed in the next section.

## V. RESULTS

The dispersion equations are solved numerically for both instability problems (with one and two boundaries). For the first problem, the instability growth rate is obtained from (26) as a function of three parameters $\theta,ka,R/a$. For the second problem, the dispersion equation is determined by (32), and the instability growth rate is obtained as a function of four parameters $\theta,ka,R/a,U_i/U_{a\,2}$ (here, $U_{a\,2}$ is the Alfvén velocity in region 2). In each plot, the instability growth rate is normalized to the quantity $\gamma^*=U_{a\,2}/a=B_2/\sqrt{4\pi\rho_1}\,a$.

Figure 2 shows the instability growth rate as a function of the magnetic shear angle $\theta$ for zero plasma velocity ($V_1=V_2=0$) and different density ratios: (a) $\rho_2/\rho_1=1$, and (b) $\rho_2/\rho_1=0.1$. The normalized curvature radii and wave number are $R/a=160$, $ka=0.15$. The ratio of the field strengths is equal to 1, $n=B_1/B_2=1$. The curves denoted by (1) correspond to the model of Rezenov and Maltsev,[3] which deals with the instability growth rate just for one boundary ($F_1$) imposing the relation between $B_0$ and $B_1$

$$B_0=B_1\sin(\theta). \tag{34}$$

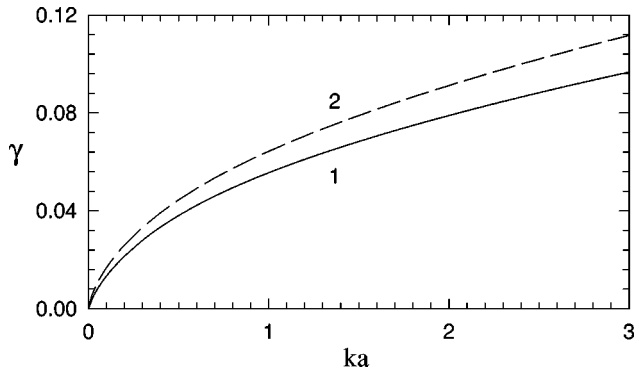


FIG. 3. Normalized instability growth rate as a function of $ka$ for $\theta=0$, $R/a=160$, $V_1=V_2=0$. The curve (1) corresponds to the case of equal densities, $\tilde{\rho}_1=\tilde{\rho}_0=\tilde{\rho}_2=1$, and the curve (2) corresponds to the case of different densities, $\tilde{\rho}_1=1$, $\tilde{\rho}_0=0.5$, $\tilde{\rho}_2=0.1$.

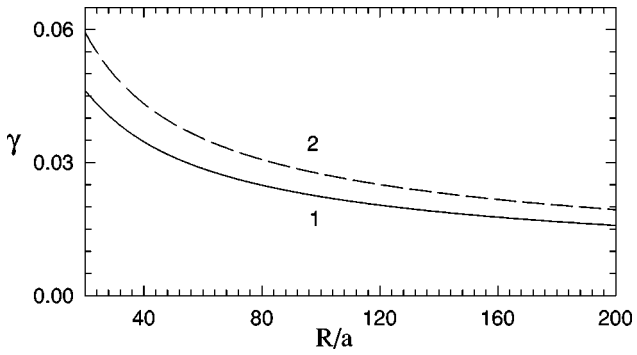


FIG. 4. Normalized instability growth rate as a function of $R/a$ for $\theta=0$, $ka=0.15$, $V_1=V_2=0$. The curve (1) corresponds to the case of equal densities, $\tilde{\rho}_1=\tilde{\rho}_0=\tilde{\rho}_2=1$, and the curve (2) corresponds to the case of different densities, $\tilde{\rho}_1=1$, $\tilde{\rho}_0=0.5$, $\tilde{\rho}_2=0.1$.

In our model, we impose another relation between $B_0$ and $B_1$

$$\mathbf{B}_0=(\mathbf{B}_1+\mathbf{B}_2)/2. \tag{35}$$

Thus, the magnetic field in the layer is determined as the vector average of the magnetic fields in regions I and II. This relation seems to be more reasonable because it is symmetric with respect to the fields $\mathbf{B}_1$ and $\mathbf{B}_2$.

In Fig. 2 the curves (2) correspond to our solution in the case of one boundary (one tangential discontinuity), while the curves denoted by number (3) correspond to our solution in the case of two boundaries. Comparing the curves (1) and (2) in Fig. 2, one can see that both models have practically the same maximum growth rate corresponding to the antiparallel magnetic fields. However, the angle interval of the instability in our model is larger than that in the model of Rezenov and Maltsev.[3] This is caused by the difference in the relations (34) and (35) used in the models. The comparison of the curves (2) and (3) shows that a finite thickness of the layer diminishes the instability rate. Comparing the plots (a) and (b), one can see that interchange instability becomes stronger for smaller density $\rho_2$.

Figure 3 shows the instability growth rate as a function of the normalized wave number $ka$ for zero velocity, antiparallel magnetic fields ($\theta=0$) with the ratio $n=1$, and the normalized curvature radius $R/a=160$. The curves (1) and (2) correspond to the different values of normalized density $\tilde{\rho}_2=1, 0.1$. One can see that the instability growth rate is a monotonic increasing function of the wave number.

Figure 4 shows the instability growth rate as a function of the normalized curvature radius for a fixed normalized wave vector $ka=0.15$, and two different cases of density ratio, $\rho_2/\rho_1=1$ [curve (1)] and $\rho_2/\rho_1=0.1$ [curve (2)]. Similar to Fig. 3, the velocities ($V_{0,1,2}$) are assumed to be zero and the magnetic fields are antiparallel ($\theta=0$) with the ratio $n=1$. One can see that the instablity growth rate is a monotonic decreasing function of a curvature radius. From Figs. 3 and 4 we can also conclude that the instability growth rate is an increasing function of the layer thickness.

Figure 5 shows the instability growth rate as a function of the normalized relative velocity $V=V_1-V_2$ for antiparallel magnetic fields ($\theta=0$). The normalized wave number and curvature radius are $ka=0.15$, $R/a=160$. Similar to Figs. 3 and 4, the curves (1) and (2) correspond to different density values, $\tilde{\rho}_2=1, 0.1$, respectively. Plots (a) and (b) correspond to parallel ($\alpha=0$) and perpendicular ($\alpha=\pi/2$) direction of the vector $\mathbf{V}$ with respect to the magnetic field.

Figure 6 shows the instability growth rate as a function of the velocity angle $\alpha$ for different values of the normalized relative velocity $V$. Here, the magnetic fields are assumed to be antiparallel; the wave number and the curvature radius are the same as those for Fig. 5. The curves (1), (2), and (3) correspond to $V=0$, 0.5, 1, respectively. The plots (a) and (b)

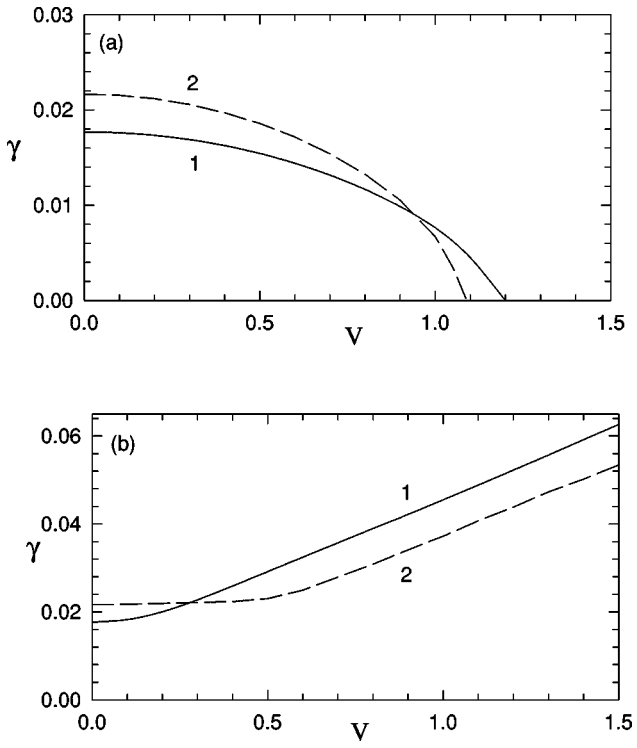


FIG. 5. Normalized instability growth rate as a function of normalized velocity $V=(V_1-V_2)$ for $\theta=0$, $ka=0.15$, $R/a=160$. The curves (1) and (2) correspond to the cases of equal ($\tilde{\rho}_1=\tilde{\rho}_0=\tilde{\rho}_2=1$) and different ($\tilde{\rho}_1=1$, $\tilde{\rho}_0=0.5$, $\tilde{\rho}_2=0.1$) densities, respectively. The plots (a) and (b) correspond to $\alpha=0$ and $\alpha=\pi/2$, respectively.

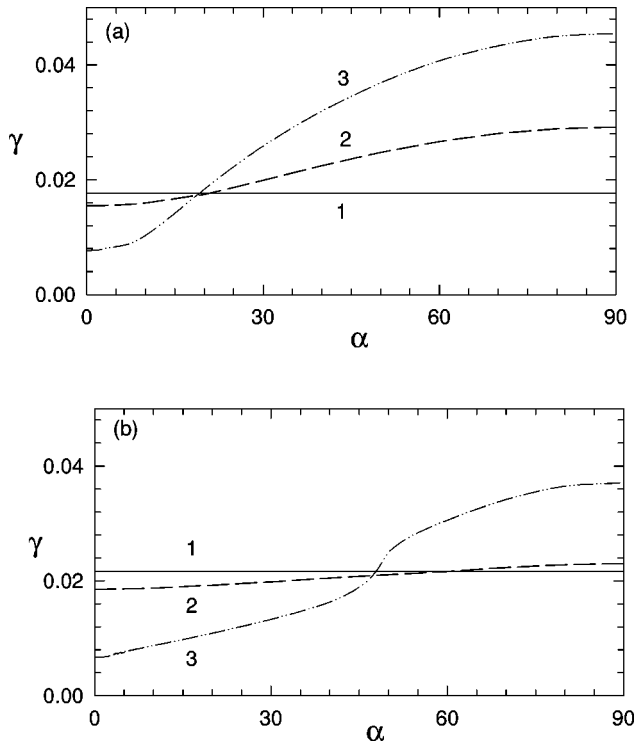


FIG. 6. Normalized instability growth rate as a function of velocity angle $\alpha$ for $\theta=0$, $ka=0.15$, $R/a=160$. The plots (a) and (b) correspond to the cases of equal ($\tilde{\rho}_1=\tilde{\rho}_0=\tilde{\rho}_2=1$) and different ($\tilde{\rho}_1=1$, $\tilde{\rho}_0=0.5$, $\tilde{\rho}_2=0.1$) densities, respectively. The curves (1), (2), and (3) correspond to different normalized velocities, $V=V_1-V_2=0$, 0.5, 1, respectively.

correspond to different density values, $\tilde{\rho}_2=1$, 0.1.

One can see from Figs. 5 and 6 that an increase of the plasma velocity component perpendicular to the magnetic field causes an enhancement of the instability growth rate. That is related to the Kelvin–Helmholtz instability acting in addition to the interchange instability. On the other hand, an increase of the plasma velocity component parallel to the magnetic field diminishes the instability growth rate. The reason is the following: For a parallel motion of the plasma, the Kelvin–Helmholtz instability is not pronounced for the velocity interval shown in the figures due to a strong magnetic field tension. And, also for small angles $\alpha$, the interchange instability growth rate is smaller because of a stabilizing role of the centrifugal force.

## VI. DISCUSSION AND CONCLUSION

The growth rate of the interchange instability is studied as a function of the magnetic shear angle, the thickness of the layer, the wave vector, and the tangential velocity of plasma.

This instability is the strongest in a case of antiparallel magnetic fields separated by the neutral layer. The instability decreases if the magnetic field of region I deviates from the direction antiparallel to the magnetic field of region II. The growth rate is positive within a finite angle interval of the magnetic shear. This angle interval of the instability is rather sensitive to the relation between the layer magnetic vector and those of regions I and II. Determining the magnetic field of the layer as a vector average of magnetic fields in regions I and II, we obtained the instability angle interval, which is twice as large as that in the model of Rezenov and Maltsev.[3]

Besides the shear angle, there are four main factors which bring about an enhanced growth rate of the interchange instability of the layer.

(1) Increase of the thickness of the layer;
(2) Decrease of the wavelength;
(3) Decrease of the local curvature radius of the layer;
(4) Plasma flow in the direction perpendicular to the magnetic field.

The instability growth rate decreases in the case of plasma flow along the magnetic field. From the physical point of view, the influence of plasma velocity can be explained in the following way. In the case of plasma flow in the direction perpendicular to the magnetic field, the interchange instability caused by the magnetic tension $B^2/R$ is enhanced by the Kelvin–Helmholtz instability which is driven by the velocity shear. But, in the case of the plasma velocity directed along the magnetic field, the Kelvin–Helmholtz modes are stabilized by the magnetic tension, and in addition, the interchange instability is also weakened by the centrifugal force, which is proportional to the velocity squared and the curvature of the surface.

Applying the results described above to conditions of the Earth's magnetopause flowed by the solar with southward interplanetary magnetic field (IMF), we find that the growth rate of the interchange instability must decrease in the meridional plane of the magnetosphere because of plasma flow along the magnetic field. On the other hand, the growth rate must increase in the equatorial plane because of plasma motion in the direction perpendicular to the magnetic field.

Taking the typical parameters: $B_2=60$ nT, $B_1=60$ nT, $n=5$ cm$^{-3}$, $a=500$ km (total width of the layer is equal to 1000 km), the relative velocity $V=0$, $R=8\cdot10^4$ km, and the wave scale $k^{-1}=3300$ km, we obtain the characteristic time of the instability as $\tau=a/(\tilde{\gamma}U_{a\,2})=48$ s for the case of the density ratio $\rho_2/\rho_1=1$, and $\tau=39$ s for the case of the density ratio $\rho_2/\rho_1=0.1$.

The instability can evolve into a nonlinear stage, if the growth time $\tau$ is much less than the time $t_c$ of plasma convection along the dayside magnetopause. Using a rough estimation of the convection time $t_c\sim R/U$ ($U\sim400$ km/s), we find the ratio $\tau/t_c\sim=0.2$. This means that the perturbations caused by the interchange instability can reach a nonlinear stage at the dayside magnetopause for southward IMF.

As shown by Luhmann *et al.*,[9] in the case of arbitrary IMF orientation, there always exist regions with antiparallel magnetic fields at the magnetopause. But, the locations of these regions are strongly dependent on the IMF direction.

For steady-state solar wind flow around the magnetosphere, the magnetic field is enhanced near the magnetopause in the boundary layer, which is thus called the magnetic barrier or plasma depletion layer (see Erkaev *et al.*[10] and references therein). In the case of nonsteady IMF variations from north to south, the magnetic field can change its direction inside the magnetic barrier. For this situation, the interchange instability theory studied above can also be ap-

plied. In such a case the thickness of the boundary layer is larger: It is on the order of the magnetic barrier thickness (a few thousand kilometers). For the same curvature radius, the instability growth rate is larger when the boundary layer is thicker.

With regard to space plasma, there is an important question concerning applicability of an MHD model for the interchange instability analysis. The MHD approach is often used for space plasma because it much easier than the kinetic study. It is generally believed that an MHD model can be used for sufficiently large scales which are much larger than plasma scales. For magnetosheath conditions, the ion scale is about 100 km. Therefore, the wave scale $1/k$ and the layer thickness $2a$ as considered in our model should exceed the plasma scale of 100 km.

It is a fact that the interchange instability growth rate obtained in kinetic study[11] for a plasma with a pressure gradient is similar to that obtained in an MHD model. This means that the physics of the interchange instability can be described in the framework of the MHD model.

Another question is that about the assumption of an incompressible plasma used in our model. We take into account a difference in densities between regions I, II, and III, but within each region the density is assumed to be constant. Perturbations of the density propagate from the magnetopause with the fast magnetosonic speed $c_{s+}$. An incompressible MHD model can be applied when the distance of the compressible wave propagation exceeds the surface wave scale, $c_{s+}\tau \gg 1/k$ (where $c_s$ is the fast magnetosonic speed and $\tau = \gamma^{-1}$). The fast magnetosonic speed is larger than the Alfvén speed, and thus the last condition is covered by the more stronger condition, $U_{a1}\tau \gg 1/k$, which can be written in dimensionless form as follows: $(B_1/B_2)ka \gg \tilde{\gamma}$. This condition is well fulfilled for the parameters used in our study.

The interchange instability of the magnetopause seems to be an important process which brings about transfer of magnetic flux tubes through the magnetopause. Finally, this might cause an enhanced magnetic field diffusion at the high shear magnetopause, which in its turn can initiate the reconnection process (see Priest and Forbes,[12] and references therein). As a trigger of magnetic reconnection for the magnetopause, the interchange instability can be considered as a complementary factor to the instabilities of a thin current sheet.[13–15]

Besides the Earth's magnetosphere, additional possible applications of our results are the magnetospheres of the other planets, and also magnetic clouds (large magnetic cavities) convected by the solar wind.

## ACKNOWLEDGMENTS

Part of this work was done during a research visit of I.L.A. and N.V.E. to Graz and H.K.B. to Krasnoyarsk. We thank Professor V. S. Semenov for fruitful discussions.

This work is supported by the INTAS-ESA Project No. 99-01277, by Grants No. 01-05-65070 and No. 01–05–02003 from the Russian Foundation of Basic Research, and by Project No. I.4/2001 from ''Österreichischer Akademischer Austauschdienst.'' It is also supported in part by the Austrian ''Fonds zur Förderung der wissenschaftlichen Forschung'' under Project No. P13804-TPH. We acknowledge support by the Austrian Academy of Sciences, ''Verwaltungstelle für Auslandsbeziehungen,'' and the Russian Academy of Sciences.

[1] S. Chandrasekhar, *Hydrodynamic and Hydromagnetic Stability* (Oxford University Press, London, 1968).
[2] J. P. Freidberg, *Ideal Magnetohydrodynamics* (Plenum, New York, 1987).
[3] B. V. Rezenov and Y. P. Maltsev, Ann. Geophys. **12**, 183 (1994).
[4] I. I. Alexeev and V. P. Maltsev, Geomagn. Aeron. **30**, 134 (1990).
[5] I. L. Arshukova and N. V. Erkaev, ''Interchange instability of the subsolar magnetopause,'' in *Solar Wind—Magnetosphere 3*, edited by H. K. Biernat, C. Farrugia, and D. Vogl (Österreichische Akademie der Wissenschaften, Vienna, 2000).
[6] L. D. Landau and E. M. Lifshitz, *Electrodynamics of Continuous Media* (Pergamon, Oxford, 1960).
[7] L. C. Lee, R. K. Albano, and J. R. Kan, J. Geophys. Res. **86**, 54 (1981).
[8] C. Uberoi, Planet. Space Sci. **34**, 1223 (1986).
[9] J. G. Luhmann, R. J. Walker, C. T. Russell, N. U. Crooker, J. R. Spreiter, and S. S. Stahara, J. Geophys. Res. **89**, 1741 (1984).
[10] N. V. Erkaev, H. K. Biernat, and C. J. Farrugia, Phys. Plasmas **7**, 3413 (2000).
[11] A. F. Alexandrov, L. S. Bogdankevich, and A. A. Rukhadze, *Principles of Plasma Electrodynamics* (Springer, Berlin, 1984).
[12] E. Priest and T. Forbes, *Magnetic Reconnection* (Cambridge University Press, Cambridge, 2000).
[13] J. Büchner and J.-P. Kuska, Ann. Geophys. **17**, 604 (1999).
[14] P. L. Pritchett, F. V. Coroniti, and V. K. Decyk, J. Geophys. Res. **101**, 27413 (1996).
[15] P. H. Yoon, A. T. Y. Lui, and H. K. Wong, J. Geophys. Res. **103**, 11875 (1998).